

Finite Element Modelling of Concrete Filled Double Skin Steel Tubular Columns under Cyclic Axial Compression Load

Riyadh J. Aziz
Civil Engineering
Department, Al-Nahrain
University, Baghdad, Iraq

Laith Kh. Al-Hadithy
Civil Engineering
Department, Al-Nahrain
University, Baghdad, Iraq

Shayma M. Resen
Civil Engineer, State Company for
Steel Industries, Baghdad, Iraq
Shayma.mohammed2@gmail.com

Abstract:

CFDSST Concrete Filled Double-skinned steel tubular columns are composite columns consisting of two concentric circular steel tubes with concrete filler in between. Finite elements method is considered through the use of the computer program ABAQUS to model CFDSST columns numerically under cyclic axial compression. Damage plasticity model was considered to model the concrete while elastic-plastic model used to model the steel tubes. six CFDSST specimens and three ordinary Concrete Filled Steel Tubular (CFST) specimens were analyzed under static axial compression, while three CFDSST specimens were considered for analysis under cyclic axial compression. The numerical results were presented in terms of axial load axial strain displacement curves. It was found that the ultimate axial load carrying capacity calculated numerically in good agreement with that of the experimentally tested specimens. Also it was concluded that Damage plasticity model used for simulating the behavior of concrete and metal plasticity model used for simulating the behavior of steel produced accurate results as compared to the experimental results.

Keywords: *CFDSST, composite columns, finite element modeling, ABAQUS.*

1. Introduction

Concrete Filled Double Skinned Steel Tubular (CFDSST) columns are composite column members consisting of two coincide circular thin steel tubes with filling-material between them have been studied for different applications. Montague et al. [1] firstly used this type of members for vessels under external pressure in very deep water, while Wei et al. [2] proposed it for compression member in offshore constructions. Recently CFDSST has been under consideration for use as high-rise piers to reduce the structure self-weight, while maintaining a large energy absorption capacity against earthquake loading. There may be a potential for concrete filled double skin tubes to be used as columns in building structures, composite piles in offshore applications and other devices to absorb energy due to the increased ductility. The confinement effect created by steel casing enhances the material properties of concrete by

putting the concrete under a triaxial state of stresses thereby increasing the strength and ductility of concrete. Additionally, the inward buckling of the steel tube is prevented by the concrete, thus increasing the stability and strength of the column as a system.

Elchalakani, et. al [3] reported that CFDSST columns have almost all the same advantages as traditional CFST members. Moreover, they have lighter weight, higher bending stiffness, and have better cyclic performance. It is also expected that CFDSST columns will have higher fire resistance capacities than their CFST counterparts. Sima et. al [4] reported that conventional concrete filled steel tube columns may be a good alternative to ordinary reinforced concrete and structural steel columns. CFST and CFDSST columns may result in a more efficient system for resisting cyclic loading than ordinary reinforced concrete columns. Steel tube confines the entire concrete section and exhibit better ductility under cyclic loading. To predict the complicated behavior of concrete filled double steel tubes column, a 3D nonlinear finite element model for the complete CFDSST column was generated using the ABAQUS finite element software package. The concrete damage plasticity model was used to evaluate the nonlinear material behavior of concrete. Suitable input material properties were provided from experimental test results for both axial and cyclic axial loading conditions. An elasto-plastic material model with a plastic part linearly increase branch was adopted for the steel tubes. The Finite elements model was compared with experimental data of axial compression tests taken from the literature, and with the experimental test conducted by Al- Hameedawi [5] as part of her experimental program. A set of CFDSST columns with both inner and outer tubes made of steel and have circular shape have been considered for analysis throughout this study, **Figure (1)**, shows a schematic view of the CFDSST specimens.

2. Finite Element Analysis of CFDSST Columns.

The basic concept of the finite element method consists of the idealization of the actual continuum as an assemblage of a finite number of discrete structural elements interconnected at

joints called nodal points. The solution steps by the finite element method can be divided into the following six basic steps (Zienkiewicz, and Taylor) [6]:

1. Discretization of the Structure
2. Selection of a Proper Interpolation or Displacement Models (Appropriate Functions).
3. Derivation of Element Stiffness Matrix and Load Vectors.
4. Assembling the Element Properties to Form Global Equation.
5. Solution for the Unknown Nodal Displacements.
6. Computation of Element Strains and Stresses

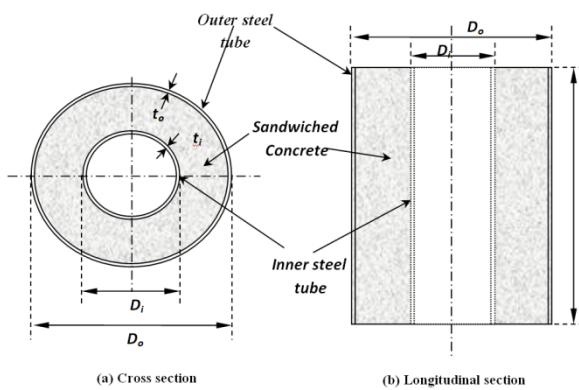


Figure (1) CFDSSST columns details, (a) cross section, (b) Longitudinal section

The three-dimensional nonlinear finite element modelling developed herein to study the behavior of concrete filled double steel tubes (CFDSSST) columns is divided in two parts:

- Geometric modeling,
- Material modeling.

Geometric modeling includes model configuration and meshing, while the material modeling includes the constitutive model used for the material modeling.

2.1 Geometric Modeling

The element library of finite element software ABAQUS is used to select the type of element. The CFDSSST column is modeled using the following ABAQUS element types:

- SC8R (8-node hexahedron continuum shell element) is used to model the steel tubes. This type of continuum shell elements are general-purpose three-dimensional stress/displacement elements for use in modeling structures that are generally slender, with a shell-like response, and three degrees of freedom at each node.
- In the modeling of the concrete and steel plates a three-dimensional eight-node

element C3D8 with three degrees of freedom at each node is used as shown in Figure(2).

A convergent study of the finite element using various element sizes for CFDST columns has been carried out. Figure (3) show three meshes of CFDST column. It is observed that all three meshes have the same axial load-axial displacement behaviour in the ascending part until it reaches to the ultimate strength and a very small difference in the descending part of the axial load-displacement curve, Figure (4) shows Axial load-axial displacement for meshes 1,2 and 3. mesh 2 is adopted in this study.

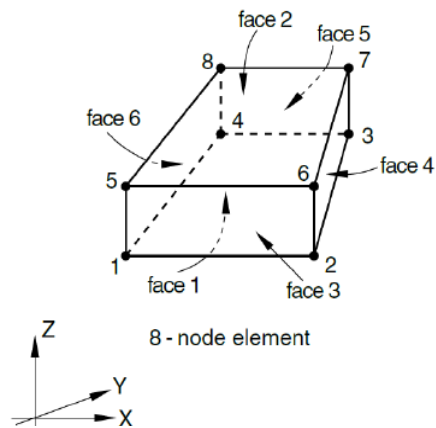
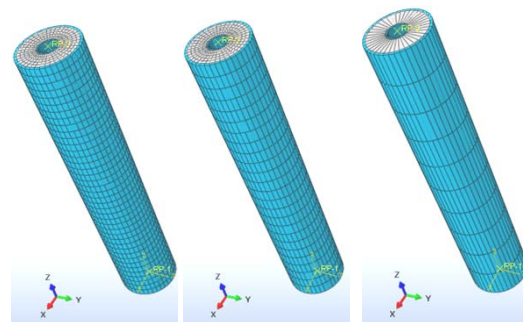


Figure (2) Three dimensional 8-node element (C3D8) used for concrete modeling, (ABAQUS Standard User's Manual, 2010) [7]



a) Mesh-1 b)Mesh-2 c)Mesh-3
Figure (3) Finite element meshes of concrete filled double steel tubes column

Mesh convergence studies were conducted to determine the optimal Finite Element mesh size that provides relatively accurate solution with low computational time. Therefore. A typical CFDSSST specimen included a total of more than 7000 elements for the concrete and the two steel tubes; Figure (4) shows the finite element discretization of the CFDSSST specimen used.

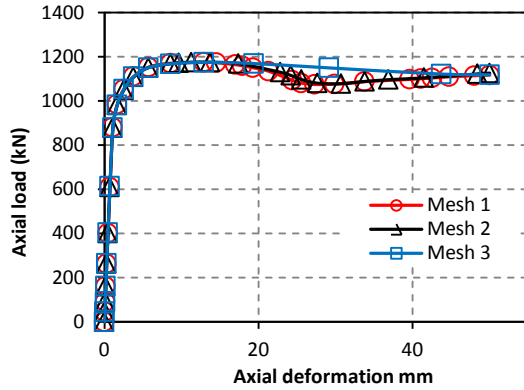


Figure (4) Axial load -axial deformation relationships for mesh 1,2 and 3

2.2 Materials Modeling

2.2.1 Modeling of Concrete

Unlike steel, concrete has different uniaxial behaviors in tension and compression and, even at the static condition; there is still a great level of uncertainty associated with material modeling of the uniaxial behavior of concrete.

It has been well documented that initial local imperfections and residual stresses have apparent influence on the behavior of hollow tubes. For CFST stub columns, however, the effects of local imperfections and residual stresses are minimized by concrete filling, and were therefore ignored in the current FE simulation. This was confirmed by the research conducted by Tao et al. [8], which explained that the out-of-plane deformation of the steel tube caused by the concrete expansion plays a similar role as the initial imperfections.

Concrete damaged plasticity (CDP) model in ABAQUS provides the ability to model the behavior of plain or reinforced concrete elements subjected to both static and dynamic loads. The model proposed by Lubliner [9] for monotonic loading and has been developed later by Lee and Fenves [10] to consider the dynamic and cyclic loadings. The model uses the concepts of isotropic damaged elasticity in combination with isotropic tensile and compressive plasticity to represent the inelastic behavior of concrete i.e. tensile cracking and compressive crushing. In addition, the stiffness degradation of material has been considered in this model for both tension and compression behaviors.

2.2.1.1. Stress Strain Relationship of Confined Concrete

Mander et al, [11] proposed a unified stress-strain approach to predict the pre-yield and post-yield behavior of confined concrete members subjected to axial compressive stress. In this approach, a concrete model for a monotonic compressive and tensile loading condition, a cyclic compressive

and tensile loading condition and cyclic reloading branches was proposed. In order to account for the confinement effects in the Finite elements model, an equivalent stress-strain curve presented in Fig. (5) was considered. Mander et al. utilized eq. (1) proposed by Popovics [12] to develop the unified stress-strain relation of the confined concrete subjected to the monotonic compression

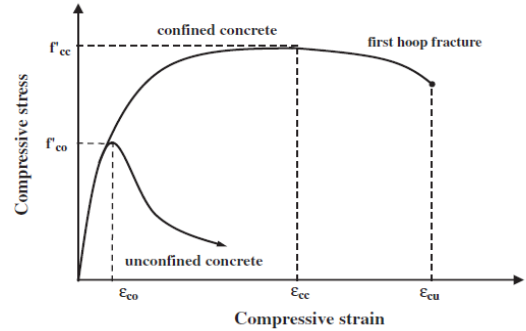


Figure (5) Confined and unconfined stress strain relations, [11].

$$f_c = \frac{f'_{cc} x.r}{r-1+(x)^r} \quad (1)$$

where:

$$x = \frac{\varepsilon}{\varepsilon_{cc}}, \quad r = \frac{E_c}{(E_c - E_{sec})}, \quad E_{sec} = \frac{f'_{cc}}{\varepsilon_{cc}}, \quad f'_c =$$

unconfined compressive stress, f'_{cc} = confined compressive stress, ε = uniaxial strain, ε_{cc} = strain at the peak concrete strength and E_c = tangent modulus of unconfined concrete. The peak strength of confined concrete f'_{cc} is calculated using the equation below [11]:

$$f_{cc} = f'_c \left(-1.254 + 2.254 \sqrt{1 + \frac{7.94f_l}{f'_c}} - 2 \frac{f_l}{f'_c} \right) \quad (2)$$

$$\varepsilon_{cc} = \varepsilon_{co} \left[1 + 5 \left(\frac{f'_{cc}}{f'_c} - 1 \right) \right] \quad (3)$$

where,

f_l = effective constant lateral confining pressure, ε_{co} = strain at peak strength of unconfined concrete.

The strain at peak strength of confined concrete (ε_{cc}) is given as a function of the strain at peak strength of unconfined concrete (ε_{co}) as equation (3). The value of ε_{co} is calculated using the relationship in equation (4). This equation was proposed by De Nicolo et al., [13] based on regression analysis of uniaxial compression tests results from 17 references, in which f'_c ranged from 10 MPa to 100 MPa.

$$\varepsilon_{co} = 0.00076 + \sqrt{(0.626f'_c - 4.33) \times 10^{-7}} \quad (4)$$

Hu and Su, [14] reported that it was found that when the diameter-to-thickness ratio of the outer tube D_o/t_o is held constant, both the ultimate strength and the lateral confining pressure f_l

decrease with the increasing of the diameter to thickness ratio of the inner tube D_i/t_i . Similarly, when the diameter-to-thickness ratio of the inner tube D_i/t_i is held constant, both the ultimate strength and the lateral confining pressure f_l also decreases with the increasing of the diameter-to-thickness ratio of the outer tube D_o/t_o . Double skin concrete-filled tubes can provide a good confining effect for concrete, especially when the diameter-to-thickness ratios of the outer and inner tubes ($D_o/t_o, D_i/t_i$) are small.

As a result of a regression analysis and parametric study, **Hu and Su, [14]**, proposed three equations (5), (6) and (7), to predict the lateral confining pressure f_l for the CFDSST columns. For practical engineering application, the minimum value of f_l predicted by these three equations could be used.

$$\frac{f_l}{f_{yo}} = 0.01791 - 0.00036 \left(\frac{D_o}{t_o}\right) - 0.00013 \left(\frac{D_i}{t_i}\right) + 0.00001 \left(\frac{D_o}{t_o}\right)^2 + 0.00001 \left(\frac{D_o}{t_o}\right) \times \left(\frac{D_i}{t_i}\right) - 0.00002 \left(\frac{D_i}{t_i}\right)^2 \geq 0 \quad (5)$$

$$\frac{f_l}{f_{yi}} = 0.01844 - 0.00055 \left(\frac{D_o}{t_o}\right) + 0.00040 \left(\frac{D_i}{t_i}\right) + 0.00001 \left(\frac{D_o}{t_o}\right)^2 + 0.00001 \left(\frac{D_o}{t_o}\right) \times \left(\frac{D_i}{t_i}\right) - 0.00002 \left(\frac{D_i}{t_i}\right)^2 \geq 0 \quad (6)$$

$$f_l = 0.525 - 0.166 \left(\frac{D_o}{t_o}\right) - 0.00897 \left(\frac{D_i}{t_i}\right) + 0.00125 \left(\frac{D_o}{t_o}\right)^2 + 0.00246 \left(\frac{D_o}{t_o}\right) \times \left(\frac{D_i}{t_i}\right) - 0.00550 \left(\frac{D_i}{t_i}\right)^2 \geq 0 \quad (7)$$

2.2.1.2 Concrete Damaged Plasticity Input Parameters

Different input data, should be defined in concrete damaged plasticity model, these key material parameters to be determined include the ratio of the second stress invariant on the tensile meridian to that on the compressive meridian (K_c), dilation angle (ψ), and strain hardening/softening rule. Other parameters include the modulus of elasticity (E_c), flow potential eccentricity (e), ratio of the compressive strength under biaxial loading to uniaxial compressive strength (f_{b0}/f'_c), viscosity parameter and tensile behaviour of concrete.

Han et al. [15], proposed constant values of 30° , 0.1, 1.16 and $2/3$ for ψ , e , K_c and f_{b0}/f'_c , respectively, while **Tao et al. [8]**, reported that constant values may not be suitable to be used in some cases and the complex nature of passively confined concrete need to be considered.

These parameters can be determined as in the following:

1. The empirical Equation (8) recommended by **ACI 318 [16]** was adopted to calculate E_c , where f'_c is in MPa.

$$E_c = 4700\sqrt{f'_c} \quad (8)$$

2. According to **Tao et al. (2013)**, default values of 0.1 and 0 can be used for the flow potential eccentricity (e) and viscosity parameter, respectively. These two parameters have no significant influence on the prediction accuracy,
3. Poisson's ratio for concrete was assumed to be 0.2.
4. Based on test data collected from 14 references, **Papanikolaou and Kappos, [17]**, proposed the following equation to predict the ratio of f_{b0}/f'_c :

$$\frac{f_{b0}}{f'_c} = 1.5(f'_c)^{-0.075} \quad (9)$$

The above equation was used in this research to determine the ratio of f_{b0}/f'_c . When the concrete strength f'_c is 30 MPa, the ratio f_{b0}/f'_c is 1.162 according to equation (9), but when f'_c increases to 100 MPa, f_{b0}/f'_c drops to 1.062. In general, the calculated ultimate strength N_u will increase slightly if a higher ratio of f_{b0}/f'_c is used, [8].

5. The ratio of the second stress invariant on the tensile meridian to that on the compressive meridian (K_c) is one of parameters for determining the yield surface of concrete plasticity model. Test results indicate that K_c varies from 0.5 to 1. The default value of K_c used in ABAQUS is $2/3$, which has been adopted by many researchers. Since f_{b0}/f'_c is expressed as a function of f'_c in Equation (9), K_c will also be related to f'_c . According to **Yu et al., [18]**, the following equation can be written to calculate K_c :

$$K_c = \frac{5.5 f_{b0}}{3f'_c + 5f_{b0}} \quad (10)$$

By introducing equation (9) into equation (10), K_c can be determined by,

$$K_c = \frac{5.5}{5 + 2(f'_c)^{0.075}} \quad (11)$$

From this equation, it can be found that K_c decreases slightly from 0.725 to 0.703 when f'_c increases from 30 MPa to 100 MPa.

6. Dilation angle (ψ) is one of parameters required for ABAQUS to define the plastic flow potential. The allowed value of ψ ranges from 0° to 56° in ABAQUS. Most researchers adopted a value of 20° or 30° for confined concrete. The dilation rate of concrete decreases with decreasing ψ , which affects the interaction between the steel tube and concrete. As pointed out by **Tao et al. [8]**, ψ is affected by the confining stress and plastic

deformation of concrete, where it decreases with increasing confinement, it is assumed that ψ is a function of the so-called “confinement factor” ξ_c . Numerical tests were conducted by **Tao** et al., [8] to identify suitable values of ψ for specimens with different ξ_c . The following equation is then proposed based on regression analysis to determine ψ for circular columns.

$$\psi = \begin{cases} 56.3(1 - \xi_c) & \text{for } \xi_c \leq 0.5 \\ 6.672 e^{\frac{7.4}{4.68 + \xi_c}} & \text{for } \xi_c \geq 0.5 \end{cases} \quad (12)$$

where the confinement factor ξ_c is expressed as:

$$\xi_c = \frac{A_s f_y}{A_c f_c} \quad (13)$$

in which A_s and A_c are the cross-sectional areas of the steel tube and concrete, respectively.

- The concrete damage plasticity model assumes two failure modes as tensile cracking and compressive crushing. ABAQUS allows to model crack propagation by using stiffness degradation. The degradation of the elastic stiffness is characterized by two damage variables, d_c and d_t , which are assumed to be functions of the plastic strains. They can take values ranging from zero, for the undamaged material, to one, for the fully damaged material. The relationship between the damage variables and the plastic strain in the concrete are shown in Figure (6). The evolution of the damage parameters adopted in this study is predicted through many repeated trials compared with the experimental results.

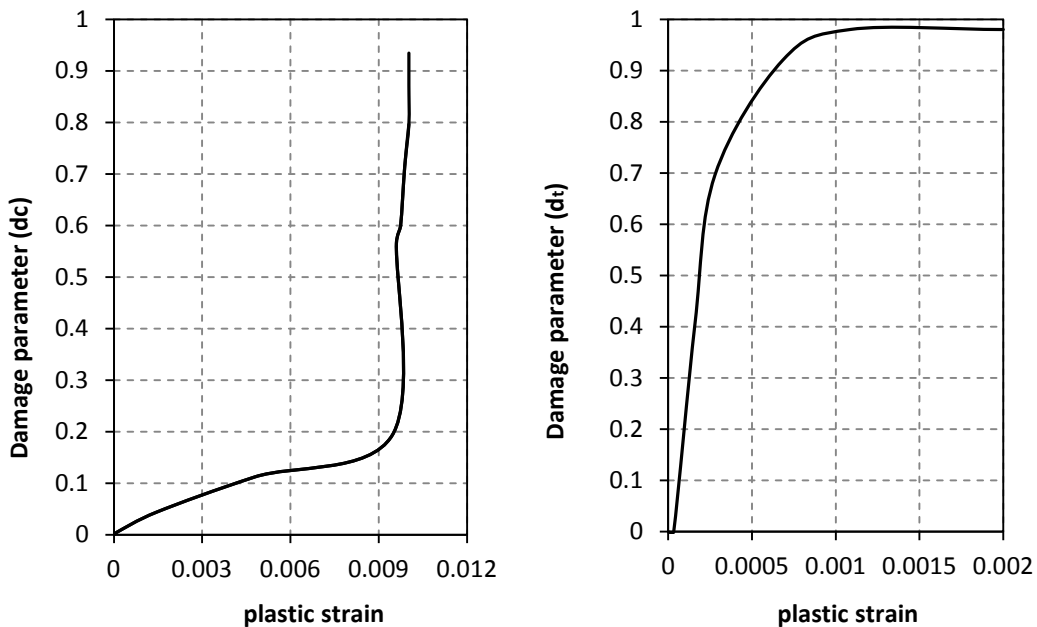


Figure (6) Damage parameters of concrete with plastic strain.

2.2.2 Modeling of Steel Tubes

An elastic-plastic model with the **Von Mises** yield criterion is used to model the constitutive behavior of steel tube. The complete stress-strain relation was obtained from uniaxial tensile tests of three longitudinal coupon specimens which tested according to the Din Standard (DIN 50125-2009) [19] as part of the experimental program conducted by Al Hameedawi [5].

In ABAQUS, three parameters are needed to defined: elastic modulus (E), yield stress (f_y), and Poisson’s ratio (ν). The elastic modulus and the yield stress were 200.0 GPa and 375.0 MPa, respectively, while Poisson’s ratio considered as 0.3.

Since the analysis of post-failure involves large inelastic strains, the engineering (nominal) stress–engineering strain curve is converted into true stress–true strain curve and implemented in the nonlinear finite element (ABAQUS) analysis. The true stress σ_{true} and true strain ϵ_{true} were calculated using the following relations [7]:

$$\sigma_{true} = \sigma_{nom} \times (1 + \epsilon_{nom}) \quad (14)$$

$$\epsilon_{true}^{pl} = \ln(1 + \epsilon_{nom}) - \frac{\sigma_{true}}{E} \quad (15)$$

where,

- σ_{true} = True stress,
- σ_{nom} = Nominal (engineering) Stress,
- ϵ_{nom} = Nominal Strain,

$$\begin{aligned} \varepsilon_{true}^{pl} &= \text{True plastic strain,} \\ E &= \text{Modulus of Elasticity} \end{aligned}$$

The proposed FE simulations considers Isotropic hardening which is generally considered to be a suitable model for problems in which the plastic straining goes well beyond the incipient yield state.

2.2.3. Boundary conditions and loading

Usually (CFDSST) columns were placed normally on the testing machine and the loads applied directly on the columns upper end and to simulate the end friction provided by the testing machine, all three translational degrees of freedom on the bottom surface $\delta_x = \delta_y = \delta_z = 0$. The top end of the CFDSST columns is fixed with $\delta_x = \delta_y = 0$ allowing displacement to take place in z direction.

The loading is applied incrementally throughout step module of ABAQUS. for axial monotonic compressive load, longitudinal prescribed displacement was applied at the nodes of the top surface of the CFDSST column, during the first step. These displacements were removed for the next step and so on for cyclic axial compressive loading, until compression failure occurred.

2.2.4. Concrete – Steel Tube Interface

There are two interfaces existed in the finite element mesh, which are the concrete to the inner tube interface and the concrete to the outer steel tube interface. Both of the interfaces are modeled by pairs of contact surfaces. The nodes on these interfaces are connected through the contact surfaces which can model infinitesimal sliding and friction between the concrete and the steel tubes. The friction coefficient used in all the analyses is $\mu = 0.25$. As a result, the nodes on the interfaces are allowed to either contact or separate but not to penetrate each other.

3. Results of the Finite Element Analysis

ABAQUS finite element program has been used in the numerical analysis of the CFDSST columns under static and cyclic loading, the finite element results were compared with well defined problem and with the experimental program conducted by Al Hameedawi [5]. The results are presented here in terms of ultimate axial strength, axial load-strain relationships, under static and cyclic loading condition.

3.1. Ultimate Axial Strengths under Static Axial Compression

A comparison between the ultimate axial strength of CFDSST specimens obtained from experimental results and finite element results is carried out. The ultimate strength obtained from the experimental tests (N_{ue}) and finite element analyses (N_{ur}) have been investigated.

Table (1) shows the details of the considered columns for comparison, also it includes the results of the ultimate loads of the concrete filled Double steel tubes (CFDSST) columns obtained by Al Hameedawi [5] through the experimental testing under monotonic loading condition, five CFDSST specimens and three CFST specimens are considered in this comparison, in addition the specimen (cc5a) which was tested by Tao et. al. [20] also been considered for comparison. It can be seen that good agreement has been achieved between the experimental and numerical results for the considered specimens. The ratio between the experimental and numerical ultimate strength for the considered columns is calculated where a maximum difference of $\pm 6\%$ between experimental and numerical results for column specimens was observed. The thickness of the outer steel tube affected the ultimate strength of the CFDSST specimens, where this strength decreased by 33% and 42% when thickness of this tube changed from 4.5 mm to 3.0 mm and from 4.5 mm to 2.0 mm, respectively. Specimen with hollowness ratio of 0.571 recorded the highest ultimate strength while below of more that this value the ultimate strength found to be less.

3.2. Axial Load-Axial Strain Curves under Static Axial Compression

The finite element analysis program ABAQUS is used to analyze CFDSST columns under axial compression; the load displacement curve of CFDSST columns predicted by the finite element program is compared to the experimental data of the specimen (cc5a) tested by Tao et al. (2004) as shown in Figure (7), properties of the specimen (cc5a) were presented in Table (1). Hu and Su [14], used the finite element computer program but with a linear Drucker-Prager model for concrete to simulate the same specimen (cc5a) tested by Tao et al. [7]. Load-axial strain of the specimen (cc5a) obtained by Hu and Su, [14] also is included in Figure (7). It is quite obvious that there is a good agreement between the finite element models of the current study and of Hu and Su [14] and the experimental test result of Tao et. al [20].

Table (1) Details, material properties and experimental and numerical ultimate axial strength of CFDSST columns

Specimen	$D_o \times t_o$ (mm)	$D_i \times t_i$ (mm)	χ	f_{yo} MPa	f_{yi} MPa	L mm	N_{ue} MPa	N_{ut} MPa	N_{ut}/N_{ue}	Tested by
cc5a	114×3.0	58×3.0	0.54	294.	375	342	904	884	0.97	Tao et al. [19]
DSM-T1-H1	114×4.5	40×3.3	0.381	375	250	600	1188	1174	0.98	Al Hameedawi [5]
DSM-T2-H1	114×2.0	40×3.0	0.363	375	295	600	632	675	1.06	Al Hameedawi [5]
DSM-T3-H1	114×3.0	40×3.0	0.37	250	295	600	838	907	1.07	Al Hameedawi [5]
DSM-T1-H2	114×4.5	60×3.8	0.571	375	375	600	1210	1192	0.98	Al Hameedawi [5]
DSM-T1-H3	114×4.5	75×3.3	0.714	375	375	600	1070	1026	0.96	Al Hameedawi [5]
SSM-T1	114×4.5	-	-	375	-	600	1252	1253	1.00	Al Hameedawi [5]
SSM-T2	114×2.0	-	-	375	-	600	727	755	1.04	Al Hameedawi [5]
SSM-T3	114×3.0	-	-	375	-	600	849	868	1.02	Al Hameedawi [5]

where,

N_{ue} = Experimental ultimate load in (MPa), N_{ut} = Numerical ultimate load in (MPa) (ABAQUS). **DS**: Double Skin, **SS**: Single Skin, **M**: Monotonic Loading, **Ti**: Thickness No. i (i=4.5,2,3), **Hi**: Hollowness ratio No. i (i=0.381,0.571,0.714 D_o : Diameter of outer steel tube, t_o : Thickness of outer steel tube, D_i : Diameter of inner steel tube, t_i : Thickness of inner steel tube, **L**: length of steel tube, χ : Hollowness ratio = $\chi = \frac{D_i}{D_o - 2 t_{so}}$

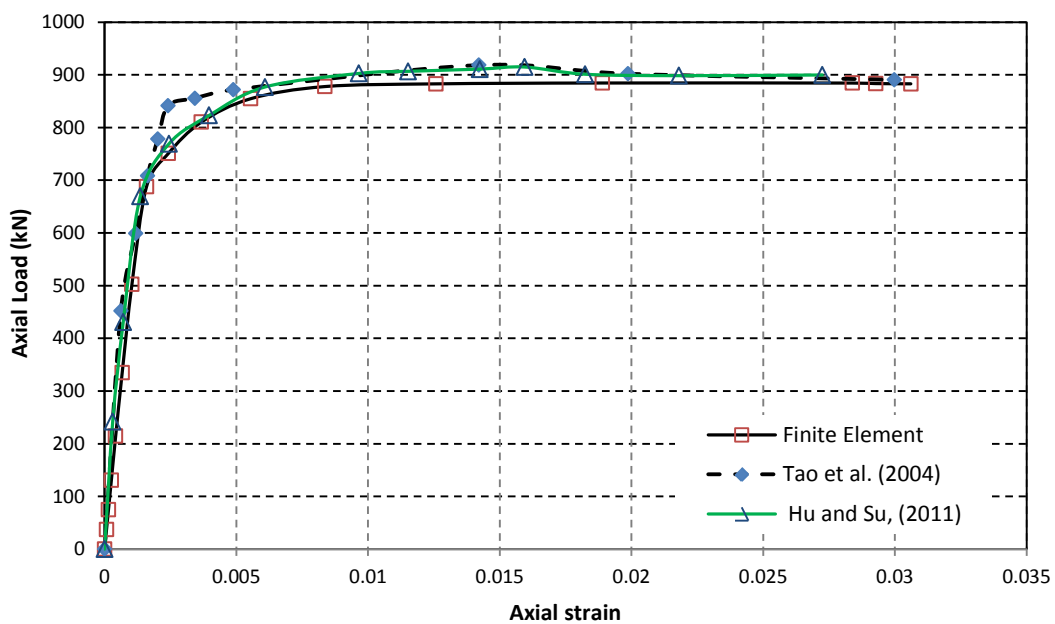


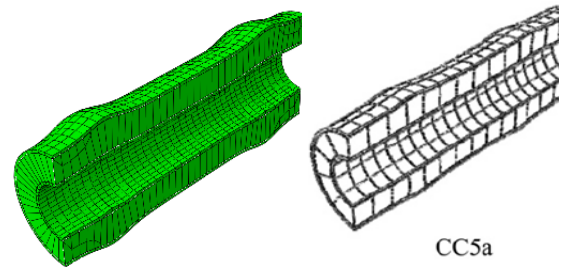
Figure (7) Comparison between numerical and experimental axial load-axial strain curves for specimen **cc5a**.

The deformation shape of the specimen (**cc5a**) has also been verified using the finite element model with that predicted by Hu and Su,[14] as shown in **Figure (8)**, where similar deformation shapes were achieved.

The eight specimens experimentally tested by Al Hameedawi [5] presented in Table (1) were considered here for another kind of comparison. Axial load-axial strain at mid-span of these specimens measured experimentally through strain gages attached to the mid-span of outer

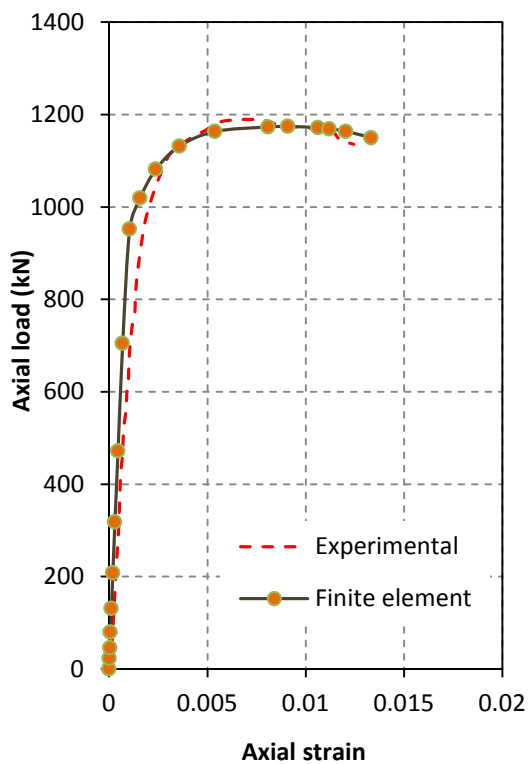
steel tubes, are compared with those determined by the finite element program ABAQUS. **Figure (9)** includes the relation of axial load and axial mid-span strain of five CFDSST specimens with three different hollowness ratios and three different outer tube thicknesses, and three CFST specimens with different outer tube thickness, numerical and experimental ultimate strength values of these specimens were presented in Table (1).

From **Figure (9)**, it can be observed that a good agreement between the experimental and numerical behavior of the considered specimens were achieved, especially in the post yield region, some difference in terms of the ultimate axial strength was recorded for the specimen DSM-T2-H1, which has the least thickness of outer steel tube. Even there is little divergence recorded after reaching the ultimate strength for some specimens, still the finite element analysis is of acceptable agreement and trust.

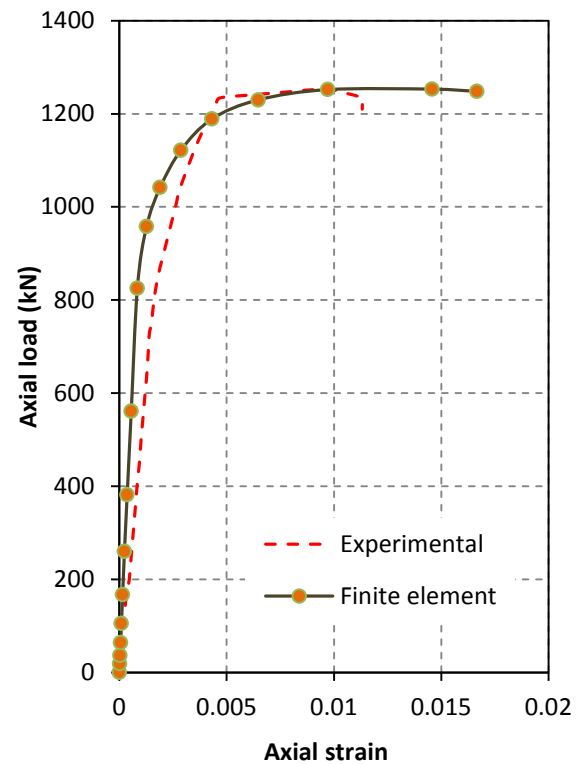


(a) Numerical Simulation by ABAQUS (b) Numerical simulation by **Hu and Su [14]**

Figure (8) Comparison between the current numerical model and the numerical simulation of **Hu and Su [14]** deflected shape for specimen **cc5a**.

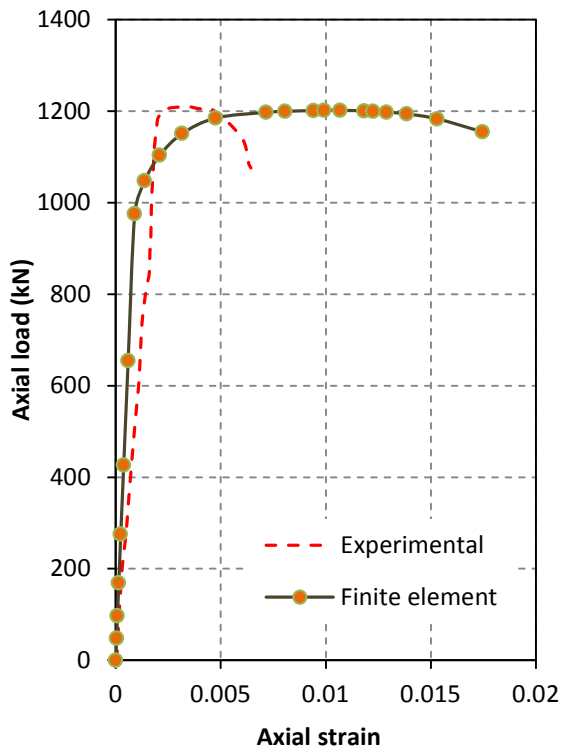


a) Axial load-axial strain of DSM-T1-H1 column

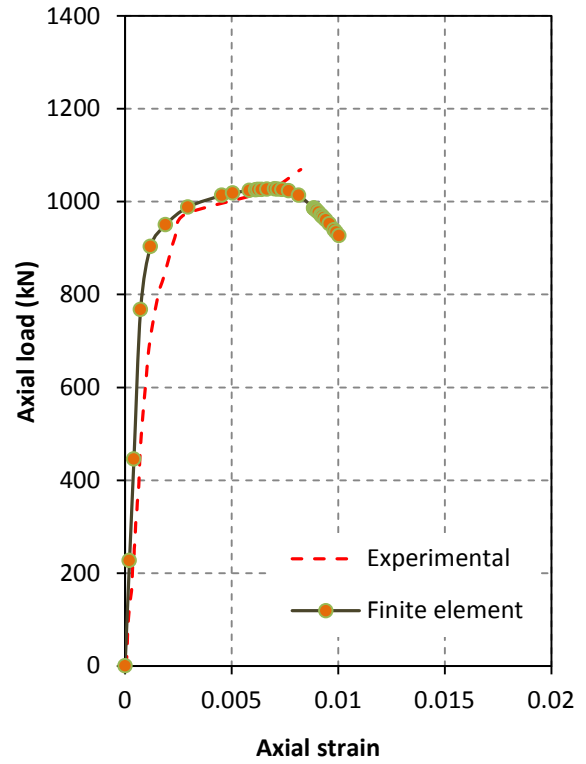


b) Axial load-axial strain of SSM-T1 column

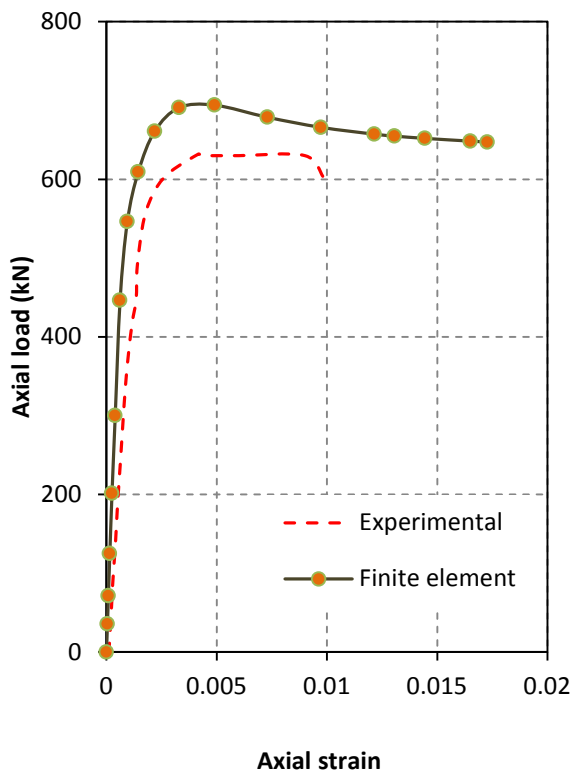
Figure (9) Comparison between experimental and finite element axial load-axial displacement curves for columns at mid span



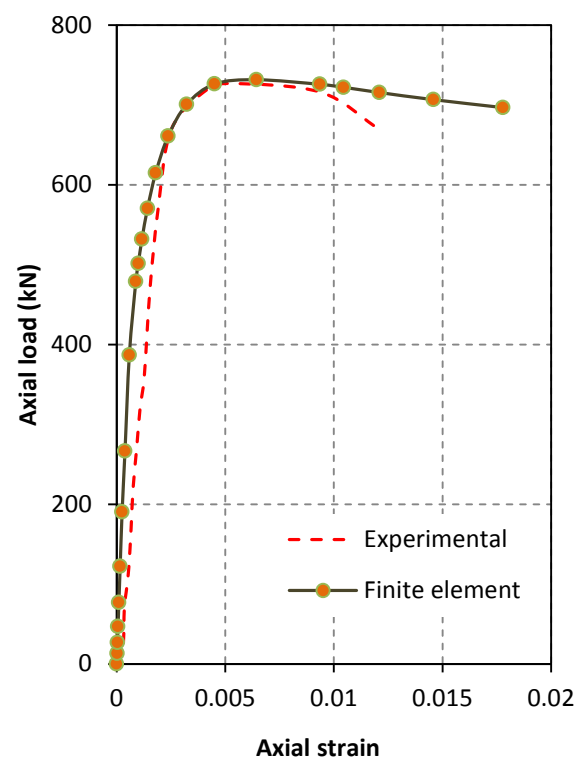
c) Axial load-axial strain of DSM-T1-H2 column



d) Axial load-axial strain of DSM-T1-H3 column

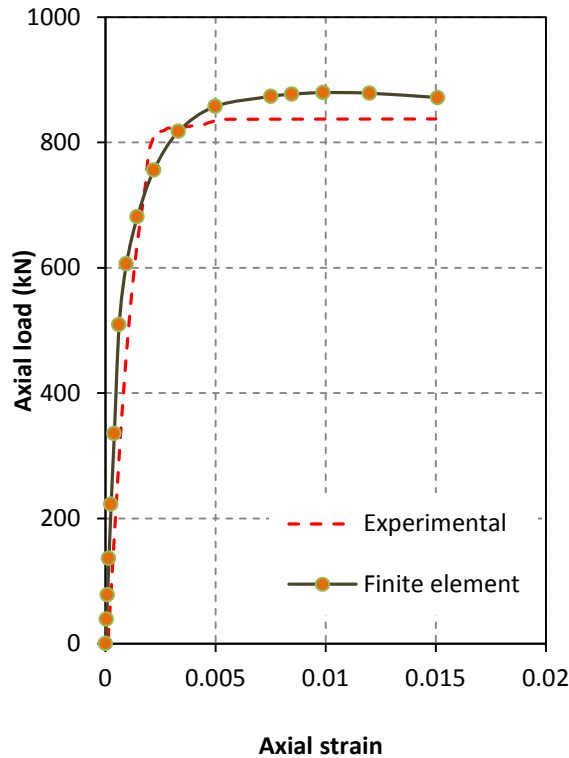


e) Axial load-axial strain of DSM-T2-H1 column

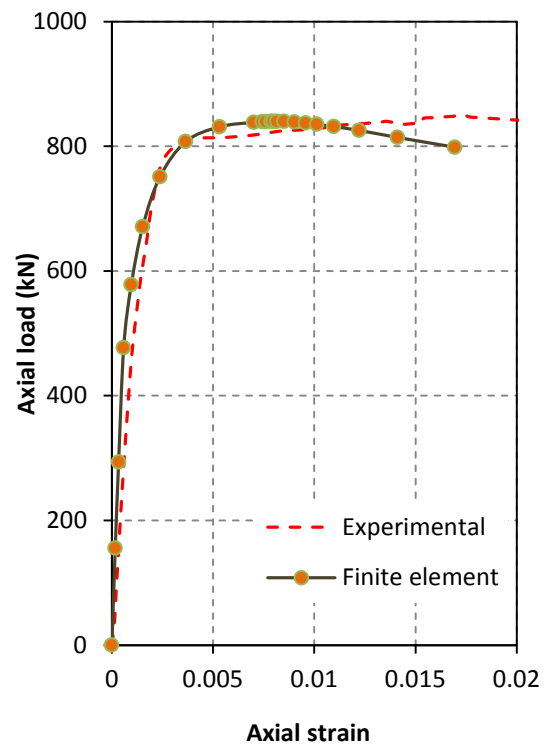


f) Axial load-axial strain of SSM-T2 column

Figure (9) Continued



g) Axial load-axial strain of DSM-T3-H1 column



h) Axial load-axial strain of SSM-T3 column

Figure (9) Continued

3.3. Axial Load-Axial Strain Curves under Cyclic Axial Compression

The second part of this study is the behavior of CFDSST under cyclic axial compression loading, the finite element program ABAQUS will also be used to implement the numerical part. The concrete damage plasticity model is also adopted in modelling the filled concrete under cyclic loading, but in the cyclic loading case a damage parameter need to be defined, this parameter is related to modeling the behavior of concrete in tension,

First the present Finite Element model is used to simulate the specimen **O7I2** which is experimentally tested by Zhao et.al. [21], under cyclic axial compression. This specimen has the properties of: outer tube diameter, thickness of outer tube, diameter of inner tube, thickness of inner tube, length, yield strength of outer tube, yield strength of inner tube, and concrete compressive strength, of $D_o=163.8mm$, $t_o=2.35mm$, $D_i=101.6mm$, $t_i=3.2mm$, $L=500mm$, $f_{yo}=395 (MPa)$, $f_{yi}=394 (MPa)$, $f'_c=63.4(MPa)$, respectively.

Axial cyclic compression with 20 cycles of 90% axial strength was applied to this specimen

after yielding occurred then the specimen loaded to failure as shown in **Figure (10)**, where acceptable agreement between the experiment of Zhao et.al. [21] and the finite element model as it recorded about 91% of the ultimate load.

The finite element model was made to simulate two specimens (DSR-T1-H1 and DSR-T1-H2) from the experimental program of Al Hameedawi [5] whose geometric and material properties are similar to DSM-T1-H1 and DSM-T1-H2 specimens, which presented in Table (1). The CFDSST specimens were subjected to variable cyclic axial compression load, through variable loading history as shown in **Figure (11)**, in these loading history different prescribed displacements were considered to be applied cyclically in the axial direction, each prescribed displacement was applied through two cycles, each cycle included (loading-unloading).

Figures (12) and **(13)** show the cyclic axial load-axial strain curves at mid span of the specimens DSR-T1-H1 and DSR-T1-H2 respectively, where reasonable agreement between the experimental and the finite element analysis can be observed.

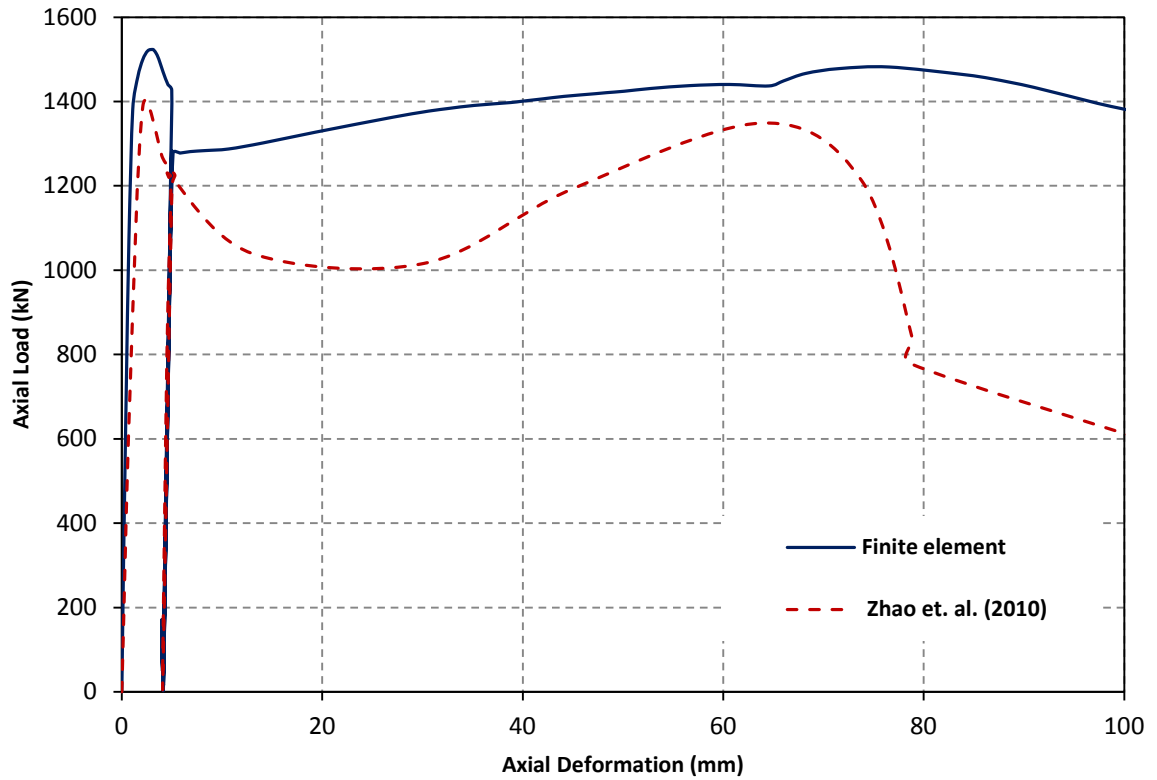


Figure (10) Numerical and experimental cyclic axial load-axial deformation curves for column O7I2 by Zhao et.al.[21].

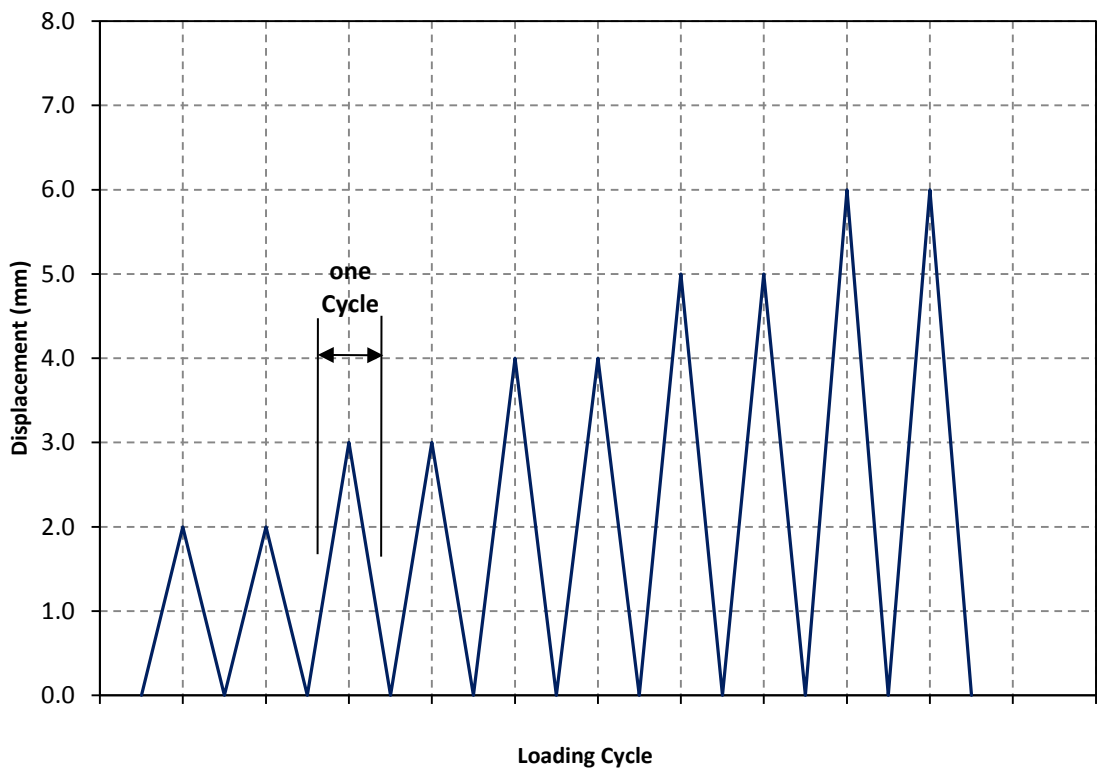


Figure (11) Loading history considered in the experimental program of Al Hameedawi [5].

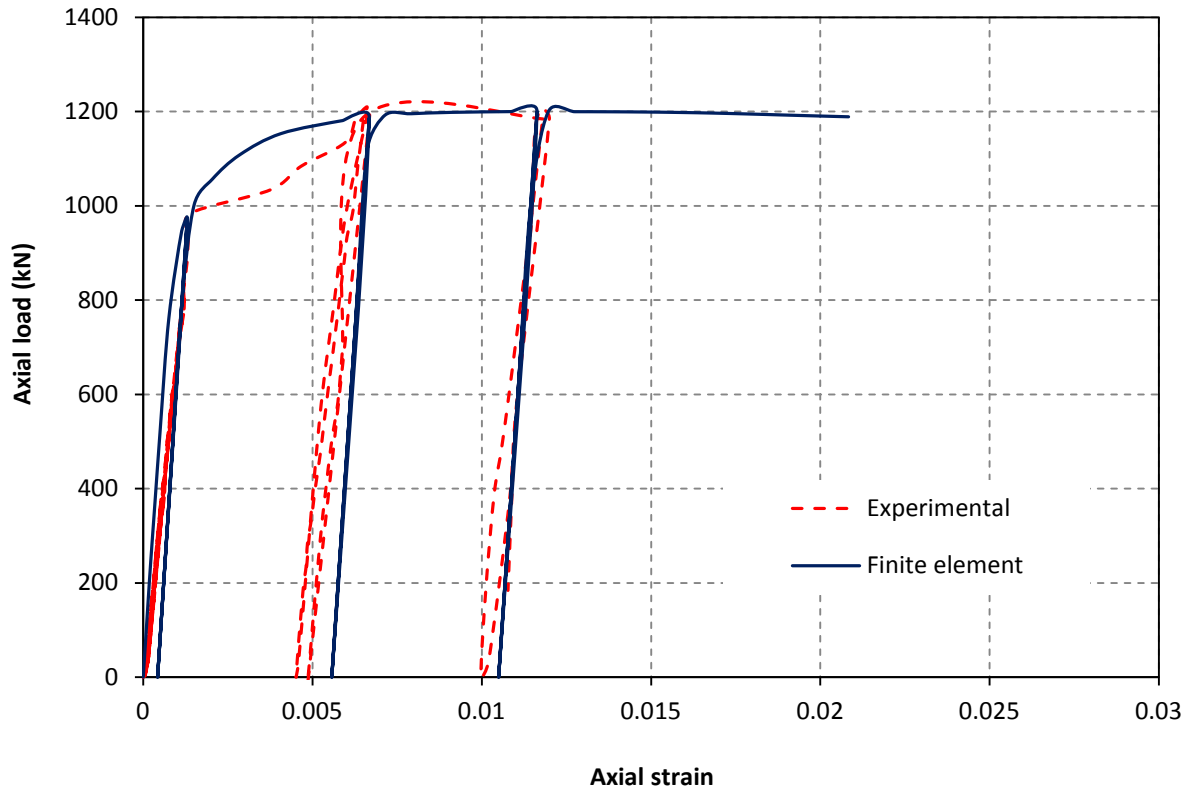


Figure (12), Finite element and experimental axial cyclic load-axial strain curves mid-span of DSR-T1-H1specimen.

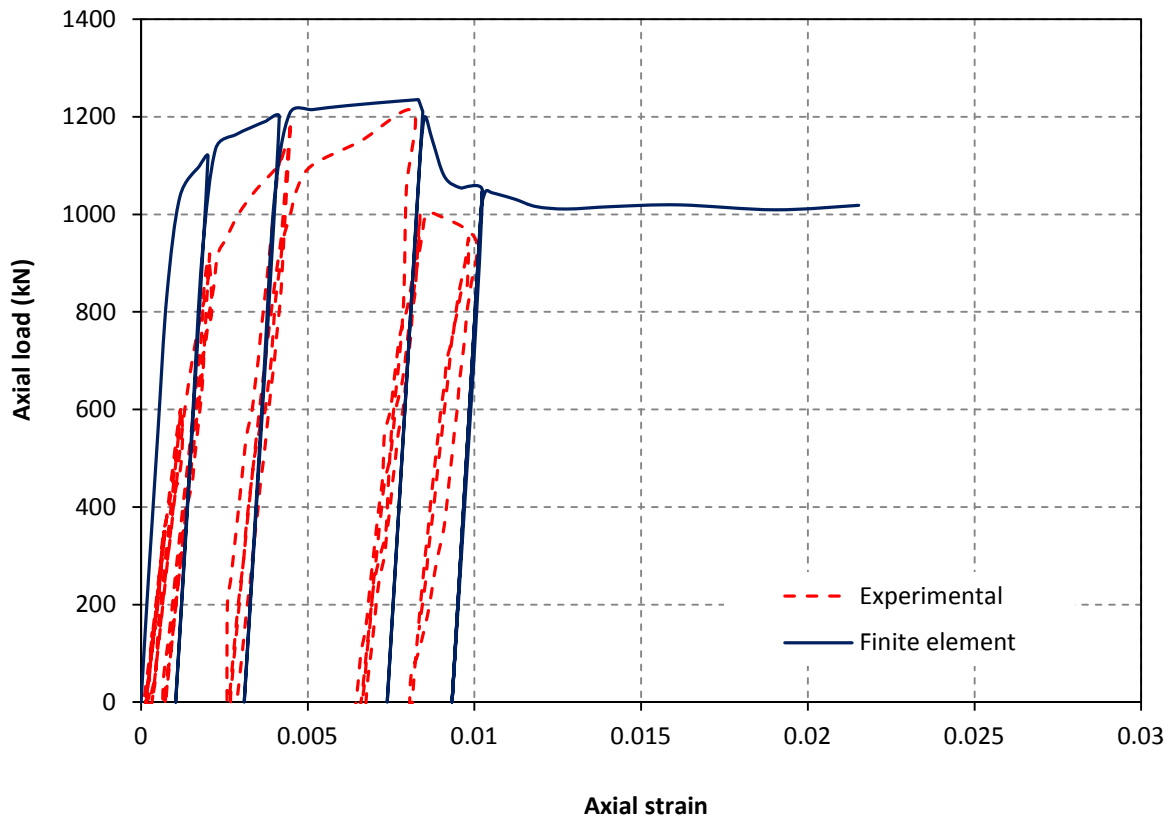


Figure (13) Finite element and experimental axial cyclic load-axial strain curves at mid-span of DSR-T1-H2 specimen.

According to the above described verifications between the finite element model and different experimental and numerical problems, whereas the finite element model showed reasonable and good agreement with these problems, this model will be considered in reanalyzing the entire experimental program and conducting parametric study of CFDSST specimens.

For the two specimens, it can be seen that during the two early loading cycles of 2mm and 3mm prescribed displacements, the outer and inner tubes did not attain residual axial strain, as the steel tube still performs as an elastic material, then after when plastic strain occurred, residual strains at mid span were recorded.

It can be observed that the paths of unloading cycles are parallel to the loading paths with small distance in between, this distance increase as the specimen started to yield. For the reloading cycle and at the early stages of loading, the path of reloading coincides with the loading path indicating the elastic behavior.

4. Conclusions

Along this study, the finite elements method through the computer program ABAQUS was utilized to analyze CFDSST columns under static and cyclic axial compression. Geometric and material modeling of this type of columns was performed and compared with the experimental results obtained from other studies. The finite element modeling of CFDSST conducted throughout this study revealed the following conclusions:

1. The Finite element method can effectively considered for simulating CFDSST columns especially when concrete modeled with the Concrete Damage Plasticity model under the action of both axial monotonic and repeated compression loadings.
2. The CFDSST column exhibited almost initial linear elastic deformations, followed by a nonlinear elasto-plastic deformation until the column reached its ultimate capacity.
3. Due to the high ductility of the CFDSST columns, the number of loading cycles before reaching the ultimate capacity was of no significance to the load-deformation relationship, while at post peak stage of loading, the effect was more pronounced.
4. Throughout the entire loading history, the unloading displacements of CFDSST specimens were increased with the decrease of the outer tube thickness, while for different values of hollowness

ratio the unloading displacement recorded close values.

5. References

1. Montague, P. (1975), "A Simple Composite Construction for Cylindrical Shells Subjected to External Pressure", *J. Mech. Eng. Sci.*, Vol. 17(2), 105-113.
2. Wei, S., Mau, S.T., Vipulanadan, C. and Mantrala, and S.K. (1995), "Performance of New Sandwich Tube Under Axial Loading: Experiment", *J. Struct. Eng.*, ASCE, Vol. 121(12), 1806-1814.
3. Elchalakani M; Zhao XL, and Grzebieta RH, (2002). "Tests on concrete filled double-skin (CHS outer and SHS inner) composite short columns under axial compression", *Thin-Wall Struct.*;40 (5):415–41.
4. Sima JF, Roca P. and Molins C., (2008), "Cyclic constitutive model for concrete". *Journal of Engineering Structures* 30(3): 695–706.
5. Al- Hameedawi, S. M, (2015), "Behaviour of concrete filled double skin tubular steel columns under static and repeated loadings", Ph D thesis, College of Engineering, University of Al Nahrain.
6. Zienkiewicz, O. C. and Taylor, R. L., (2000), "The Finite Element Method", Fifth edition, Published by Butterworth-Heinemann, Volume 3: Fluid Dynamics.
7. ABAQUS Standard User's Manual (2010), Version 6.10. Providence, RI (USA):Dassault Systèmes Corp.
8. Tao, Zhong, Wang , Z-B, Yu Q, (2013), "Finite element modelling of concrete-filled steel stub columns under axial compression", *Journal of Constructional Steel Research* 89 , 121–131
9. Lubliner, J., Oliver, J., Oller, S., and Onate, E., (1989), "A plastic-damage model for concrete", *International Journal of Solids and Structures*, Vol. 25, No. 3, pp. 299-326
10. Lee, J., and Fenves, G., (1998), "Plastic-damage model for cyclic loading of concrete structure", *Journal of Engineering Mechanics*, Vol. 124, No. 8, pp. 892-900
11. Mander, J.B., Priestley, M.J.N., and Park, R. (1988). "Theoretical Stress-Strain Model for Confined Concrete" *Journal of Structural Engineering*, ASCE, V.114, No. 8, p. 1827-1849.
12. Popovics, S. (1973). "A Numerical Approach to the Complete Stress-Strain Curves of Concrete." *Cem. Concr. Res.*, 3(5), 583-59.
13. De Nicolo B, Pani L, Pozzo E., (1994), "Strain of concrete at peak compressive stress for a wide range of compressive strengths", *Materials and Structures*, Volume 27, Issue 4, pp 206-210

14. Hu H.-T., and Su F.-C., (2011), "Nonlinear analysis of short concrete-filled double skin tube columns subjected to axial compressive forces" *Journal Marine Structures* 24, 319–337, Elsevier Ltd.
15. Han T. H.; Stallings J. M., and Kang Y. J., (2010), "Nonlinear concrete model for double-skinned composite tubular columns". *Construction and Building Materials* 24(12): 2542–2553
16. American Concrete Institute (ACI), (2014), "Building Code Requirements for Reinforced Concrete", ACI-381-14.
17. Papanikolaou VK, and Kappos AJ, (2007), "Confinement-sensitive plasticity constitutive model for concrete in triaxial compression", *International Journal of Solids Structures* ;44(21):7021–48.
18. Yu T, Teng JG, Wong YL, and Dong SL.,(2010), "Finite element modeling of confined concrete-I:Drucker–Prager type plasticity model. *EngStruct.*, ;32(3):665–79.
19. DIN 50125-2009, "Testing of metallic materials - Tensile test pieces", German Institute for Standardization (DIN)
20. Tao, Zhong; Han, Lin-Hai; and Xiao-Ling Zhao, (2004),"Behaviour of concrete-filled double skin (CHS inner and CHS outer) steel tubular stub columns and beam-columns", *Journal of Constructional Steel Research* 60 (2004) 1129–1158, Elsevier Ltd.
21. Zhao X. L., Tong L.W., and Wang X. Y., (2010)," CFDST stub columns subjected to large deformation axial loading", *Engineering Structures* 32,692-703, Elsevier Ltd.

6. List of Symbols

A_c	Cross sectional area of Concrete	f_{yo}	Yield stress of Outer Steel tube
A_{so}	Cross sectional area of outer steel tube Steel	f_{yi}	Yield stress of Inner Steel tube
A_{si}	Cross sectional area of Inner steel tube Steel	f_l'	Effective constant lateral confining pressure
c_3	Effective rigidity for axial compression composite member	I_s	Moment of inertia of steel
D_o	Diameter of Outer steel tube	I_c	Moment of inertia concrete
D_i	Diameter of inner steel tube	K_c	The ratio of the second stress invariant on the tensile meridian to that on the compressive meridian
d_c	Compression damage variable	L	length of steel tube
d_t	Tension damage variable	N_{ue}	Experimental ultimate load
D	Diameter of cylinder	N_{ut}	Theoretical ultimate load (ABAQUS).
d_s	Outer diameter of circular hollow steel section	N_u	Ultimate load capacity
ϵ_{nom}	Nominal Strain	N_z	Normalized axial strength Factor, $N_z = \frac{N_u}{N_o}$
ϵ	Uniaxial strain	t	Thickness of hollow steel section
ϵ_{cc}	Strain corresponding to f_{cc}	t_o	Thickness of Outer steel tube
ϵ_{co}	Axial compressive strain of concrete corresponding to f_c'	t_i	Thickness of inner steel tub
ϵ_{true}^{pl}	True plastic strain	σ_{true}	True stress
E_c	Modulus of elasticity of concrete	σ_{nom}	Nominal (engineering) Stress
E_s	Modulus of elasticity of steel	μ	Coefficient of friction
E_{oty}	Modulus of elasticity of outer tube	ν_s	Poisson's ratio for steel
E_{sec}	Secant modulus of confined concrete at peak stress, given by $E_{sec} = \frac{f_{cc}}{\epsilon_{cc}}$	ν_c	Poisson's ratio for concrete
f_{cc}	Confined compressive strength of concrete	ξ_c	Confinement factor
f_c'	Unconfined compressive strength of concrete	χ	Hollowness ratio
f_l	Confinement pressure	ψ	Dilation angle measured in the p–q plane at high confining pressure
		[ke]	Stiffness matrix

{ue}	Nodal displacement vector	{ε}	Strain vector
{re}	Nodal force vector	{σ}	Stress vector
[K]	Global stiffness matrix	{u}	Nodal displacement vector
{U}	Global nodal displacement vector	[B]	Strain - displacement matrix
{R}	Global nodal force vector	[D]	Strain-stress matrix

تمثيل سلوك الاعمدة الفولاذية الانبوبية ثنائية القشرة المملوءة بالخرسانة تحت حمل شاقولي دوري بطريقة العناصر المحددة

د. شيماء محمد رسن
الشركة العامة للصناعات الفولاذية /
وزارة الصناعة والمعادن

أ.م.د ليث خالد الحديثي
قسم الهندسة المدنية
جامعة النهريين

أ.م.د رياض جواد عزيز
قسم الهندسة المدنية
جامعة النهريين

الخلاصة:

الاعمدة الفولاذية ثنائية القشرة المملوءة بالخرسانة CFDSST هي نوع من الاعمدة المركبة، حيث انها تتكون من أنبوبين حديدين خارجي وداخلي وفراغ بينهم يملئ بالخرسانة. في هذا البحث يتم دراسة سلوك الاعمدة الفولاذية ثنائية القشرة المملوءة بالخرسانة تحت الاحمال الدوريه العموديه بطريقة العناصر المحدده باستخدام البرنامج ABAQUS، حيث تم استخدام موديل التضرر للندن للخرسانة والموديل المرن- اللدن للأنابيب الفولاذية، ستة نماذج (CFDSST وثلاثة نماذج (CFST) تم تحليلها تحت تأثير الحمل الشاقولي الساكن وثلاثة نماذج تحت تأثير الحمل الشاقولي الدوري. عرضت النتائج التحليلية من خلال علاقات الحمل والازاحة العمودية. وجد من خلال هذا البحث ان النتائج العملية موافقه مع نتائج البحث وايضا ان الموديل المستخدم لتمثيل الاعمدة تحت تأثير الحمل العمودي الدوري يعطي نتائج جيده من خلال مقارنتها مع النتائج العملية.